Modeling the Gouy-Chapman diffuse capacitance with attractive ion-surface interaction

Doblhoff-Dier, K.; Koper, M.T.M.

THE JOURNAL OF PHYSICAL CHEMISTRY C
A JOURNAL OF THE AMERICAN CHEMICAL SOCIETY

pubs.acs.org/JPCC

Article

Modeling the Gouy–Chapman Diffuse Capacitance with Attractive Ion–Surface Interaction

Katharina Doblhoff-Dier* and Marc T. M. Koper*

Cite This: J. Phys. Chem. C 2021, 125, 16664–16673

Read Online

ACCESS | Metrics & More | Article Recommendations | Supporting Information

ABSTRACT: The interfacial capacitance of a metal electrode in contact with a dilute electrolyte is generally expected to follow the behavior predicted by the Gouy–Chapman–Stern model. Recent experiments [*Angew. Chem. Int. Ed.* **2020**, *59*, 711], however, have shown that a deviation from the Gouy–Chapman behavior is observed even in dilute electrolytes on platinum and gold single-crystal electrodes. Such deviations are usually attributed to an interaction between the surface and the electrolyte ions. However, a quantitative model showing that the strong deviations from the Gouy–Champan behavior observed for Pt can be ascribed to such an effect is still lacking, particularly as other experimental observables do not indicate a strong ion adsorption. Here, we propose a double-layer model that is capable of reproducing the main experimental findings in a simple and (in parts) analytical way. The analytical model thereby includes the attractive ion–surface interaction via an additional capacitive element connected in parallel to the Gouy–Chapman capacitance. By comparing the model predictions to experiment, we subsequently infer characteristics of the ion–surface interaction. In particular, we find that the model predicts the attractive interaction to be weak (weaker than a typical chemical bond formed when contact adsorbing) and that the interaction has to be very similar for all ions. Furthermore, for a good agreement with experiment, ion-size effects are suggested to play a role in determining the potential of minimum capacitance.

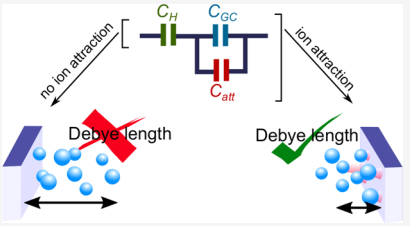

1. INTRODUCTION

When bringing an electrode into contact with an electrolyte, an electric double layer is formed. This structure of charges, countercharges, and solvent molecules determines the relationship between the surface charge and potential at the electrode, which can be expressed as the capacitance of the electrified interface. The classical model for the electric double layer at the metal–electrolyte interface in the absence of charge transfer reactions is the Gouy–Chapman–Stern model. In this model, the double-layer capacitance is described by two separate capacitors connected in series, as shown in Figure 1a and expressed in the following equation

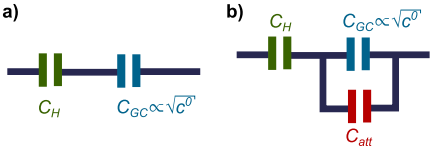

Figure 1. Equivalent circuits: (a) Gouy–Chapman–Stern model and (b) extension to account for an attractive interaction between the ions and the electrode. See eq 10.

$$\frac{1}{C} = \frac{1}{C_H} + \frac{1}{C_{GC}} \tag{1}$$

where C_H is the inner layer or Helmholtz capacitance and C_{GC} is the diffuse layer capacitance, also known as Gouy–Chapman capacitance. Traditionally, The Helmholtz capacitance is attributed to the fact that (hydrated) ions cannot access the surface too closely. In reality, it also encompasses effects of the electronic structure of the surface and its polarization, as well as solvent. Consequently, it is expected to depend on the type of anions and cations and on the charge on the electrode.[1] The diffuse layer capacitance, on the other hand, is expected to be independent of the nature of the ionic species in the electrolyte and to depend solely on the ionic charges, the ionic strength, and the applied potential. An expression for the diffuse capacitance can be derived when representing ions as point-like, charged, but otherwise non-interacting, particles in a mean-field approximation. This leads to the expression of the Gouy–Chapman capacitance

$$C_{GC}(\phi^s) = \varepsilon_r \varepsilon_0 \frac{1}{\lambda_D} \cosh\left(\frac{ze_0(\phi^s - \phi(q=0))}{2k_B T}\right) \tag{2}$$

as a function of the potential ϕ^s at the Stern or Helmholtz layer versus the potential of zero charge $\phi(q = 0)$ (pzc). The expression mentioned above is given in SI units and is valid for a 1:1 electrolyte with ion charges $\pm z$, ε_r denotes the solvent's

Received: March 16, 2021
Revised: July 2, 2021
Published: July 21, 2021

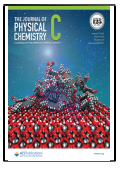

https://doi.org/10.1021/acs.jpcc.1c02381
J. Phys. Chem. C 2021, 125, 16664–16673

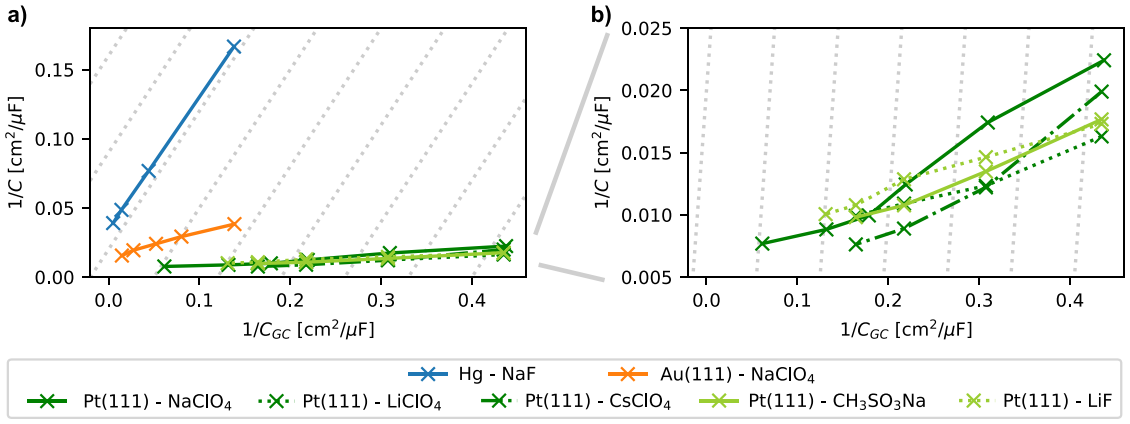

Figure 2. Parsons−Zobel plots obtained in experiments at pH = 3 for Au,[5] pH = 4 for Pt,[5,7] and pH = 7.1 for Hg.[1] Panel (b) shows a zoomed-in version of panel (a), focusing on the region of interest for Pt(111). Dotted gray lines: slope = 1, corresponding to the predictions of the Gouy−Chapman−Stern model (data for Au and Pt are reproduced from ref 5 with additional data added from ref 7; data for Hg are taken from ref 1).

relative permittivity, ε_0 is the vacuum permittivity, k_B is the Boltzmann constant, and T is the temperature. $1/\lambda_D$ is the inverse Debye length, which is proportional to the square root of the bulk concentration c^0: $\frac{1}{\lambda_D} = \sqrt{\frac{2(ze_0)^2 c^0}{\varepsilon_r \varepsilon_0 k_B T}}$. As a consequence of the square root dependence of $1/\lambda_D$ on the bulk concentration, the Gouy−Chapman capacitance decreases with decreasing electrolyte concentration, while the cosh term in eq 2 causes the Gouy−Chapman capacitance to increase exponentially as the potential ϕ^s starts to deviate from $\phi(q = 0)$. As the overall capacitance C is determined by the lower of the two capacitors C_H and C_{GC}, C_H will dominate the overall capacitance at high ion concentrations and potentials far from the pzc, while C_{GC} will be decisive at low ion concentrations near the pzc.

The approximations made in deriving the Gouy−Chapman capacitance are expected to break down at high ion concentrations due to the atomic scale structure of the interface, ion crowding,[2] layering effects,[3] and ion pair formation.[4] In dilute electrolytes and in the absence of charge transfer reactions, however, the Gouy−Chapman−Stern theory is usually expected to hold, an expectation that is largely based on the seminal work by Grahame from 1954[1] demonstrating the agreement of Gouy−Chapman−Stern theory with experimental measurements for the double-layer capacitance of a mercury electrode in a NaF electrolyte.

Recent experiments,[5] however, show a dramatic deviation of the experimentally measured capacitance from the expectations of Gouy−Chapman−Stern theory for Pt(111) and Au(111) electrodes in contact with a $NaClO_4$ electrolyte even at very low ion concentrations and in a potential window in which the surfaces are usually considered to be ideally polarizable.[6] In particular, the capacitance at low bulk ion concentrations was found to depend approximately linearly on the square root of the ion concentration (as expected by Gouy−Chapman theory) but to be higher than expected. As a consequence, the apparent Debye length as a function of ion concentration appears to be strongly reduced compared to the predictions from Gouy−Chapman theory, leading to a reduced slope in the so-called Parsons−Zobel plots, as shown in Figure 2.

Similar observations have been made earlier by Parsons and Zobel[8] for a KCl electrolyte in contact with a Hg electrode and by Eberhardt et al.[9] for $HClO_4$ and KPF_6 on gold single crystals.

Reduced slopes in the Parsons−Zobel plots can often be attributed to surface roughness, which can cause an overproportional decrease of the apparent Debye length.[10] For the single crystalline surfaces mentioned above, however, such effects cannot explain the strongly reduced apparent Debye length observed experimentally.

An alternative explanation for the reduced apparent Debye length is the presence of (weak) ion adsorption to the interface, as was put forward by the groups of Parsons[8] and Schmickler.[9] However, a quantitative model that could corroborate this explanation is still lacking. Specifically, the question arises whether ion adsorption can really cause such a strong effect on the Parsons−Zobel slope, while being weak enough such as not to cause other measurable ion adsorption effects. Neither Na^+ nor ClO_4^- is known to adsorb specifically on Pt(111). Furthermore, similar to the case on Au,[9] no shift of pzc with ion concentration is observed for $NaClO_4$ on Pt(111),[5] while this would be expected in the case of strong ion adsorption.[9] It is therefore interesting to ask two questions: (i) "Can an attractive ion−surface interaction explain the reduced Pasons−Zobel slopes, while being in line with other experimental observations?" and (ii) "Which statements can we make on the strength and nature of the ion−surface interaction?". To answer these question, we propose a simple model here that can capture the experimental observations and that allows us to make some statements on the nature of the interaction.

A valid quantitative model should address several experimental observations. In particular, it should

1. Reproduce the strongly reduced slopes observed in the Parsons−Zobel plots for Pt and, to a lesser extent, for Au (see Figure 2a).
2. Predict the potential of the minimum capacitance to lie close to the potential of zero charge for ∼0.1 mM $LiClO_4$, $NaClO_4$, $CsClO_4$, LiF, and CH_3SO_3Na electrolyte solutions (see refs 5 and 7).
3. Predict similar slopes in the Parsons−Zobel plots for Pt(111) electrodes in contact with $LiClO_4$, $NaClO_4$, $CsClO_4$, LiF, and CH_3SO_3Na electrolyte solutions[7] (see Figure 2b).
4. Allow for the potential of the minimum capacitance to shift by a few tens of mV to more negative potentials for $LiClO_4$, to stay constant for $NaClO_4$, and to shift to more positive potentials for $CsClO_4$ with increasing ionic strength (see ref 7).

https://doi.org/10.1021/acs.jpcc.1c02381
J. Phys. Chem. C 2021, 125, 16664−16673

Based on the model that we suggest in Section 2, we will be able to make several interesting and maybe somewhat unexpected statements about the nature of the interaction. Most importantly, we predict the ion−surface attraction to be rather weak, on the order of a few tens of meV and thus significantly lower than typical bond strengths for contact adsorption. Second, we predict that all ions have a very similar ion−surface attraction strength and that likely both anions and cations interact with the surface. Both observations are not in line with the classical picture of anion−surface adsorption and thus suggest a different cause for the decreased Parsons−Zobel plots for Pt(111). Although we cannot give a final answer as to the origin of the predicted interaction, we conjecture (based on yet other observations) that the solvated ion size influences the interaction.

In the following, we will first introduce our model in Section 2 and will then analyze the predictions the model makes depending on its parameters in Section 3. In doing so, we purposefully refrain from fitting the experimental results, as this would likely lead to overfitting, and focus instead on the qualitative and semiquantitative effect that different model parameters have.

2. METHODS

In our model, we introduce an extension to the Gouy−Chapman−Stern theory that allows for the inclusion of an attractive ion−surface interaction. The reason for introducing such an attractive interaction in order to capture the experimental results, rather than other effects that go beyond the classical Gouy−Chapman−Stern model, will be discussed first. In the remainder of the chapter, we introduce our model and a simple analytical approximation thereof.

2.1. Ion−Surface Attraction as a Cause for Reduced Parsons−Zobel Slopes. The Gouy−Chapman−Stern theory is based on many approximations. Consequently, it may not be immediately obvious why ion adsorption is expected to be the key factor explaining the deviations from the Gouy−Chapman−Stern theory observed for Pt[5] and Au.[5,9] To clarify this, we will briefly discuss which other approximations made in the Gouy−Chapman theory *cannot* explain an apparently reduced Debye length at low concentrations.

2.1.1. Constant ε_r. In Gouy−Chapman theory, it is assumed that ε_r is constant throughout the entire electrolyte region. In reality, ε_r typically decreases close to the surface due to surface−water interactions, Pauli repulsion of electrons, saturation effects, and/or ion crowding. One could, however, also postulate an increase in ε_r close to the surface due to a broken hydrogen bonding network at the surface and/or spilling of surface charges.[11] Such a local increase in ε_r could explain a reduced apparent screening length, albeit at high concentrations (i.e., short Debye lengths) only.

2.1.2. Ions Are Point-like and Do Not Form Ion Pairs. These approximations break down at high electrolyte concentrations and for high surface charges. At very low ion concentrations, however, and at potentials close to the pzc, as considered in the experimental measurements in Figure 2, these approximations can be expected to hold. Moreover, correcting for these shortcomings has been observed to lead to an increased screening length[2−4] rather than a decreased screening length as required here.

2.1.3. Solvent Molecules Act Exclusively as Dielectric Medium. Pajkossy and Kolb[6] previously proposed this assumption to break down by assigning a peak in capacitance observed close to pzc on Pt(111) to water reorganization—an assumption that has been backed by computational results.[12] More recent computational results suggest a capacitance peak for Pt(111) to arise from a negative capacitance stemming from the field-dependent adsorption of water to the surface with a dipole moment opposite to the field direction.[11] While such processes lead to an increase in capacitance, similarly to a reduced apparent Debye length, both processes are expected to be driven by a change in electric field at the surface rather than by a change in potential drop in the diffuse layer. The change in water-induced potential drop $\mathrm{d}(\Delta\phi)$ caused by an infinitesimal change in surface charge $\mathrm{d}Q$ at pzc should therefore be independent of the ion concentration determining the diffuse layer potential drop. Consequently, the adsorption of interfacial water close to pzc should cause an ion concentration-independent offset in $1/C$ and cannot cause a reduced slope in the Parsons−Zobel plots, which would require ion concentration dependence. We therefore exclude water flipping or water adsorption as a possible cause for the experimental results discussed here.

2.1.4. Ions Are Inert and No Charge Transfer Occurs. Partial charge transfer between ions and metal may play a role. However, experimentally, only the electrosorption valency is an observable, which is a convolution of the ion distance from the surface and the charge transfer. Therefore, one may argue that mean-field models can effectively account for such an effect by allowing the charges to approach the surface more closely than they actually do. This would lead to a reduced distance of the Stern layer from the electrode and would manifest itself in a change in the Helmholtz-like contribution to the capacitance without influencing the slope in the Parsons−Zobel plots.

2.1.5. Ion−Surface Attraction. While all of the above-mentioned effects seem to be incapable of causing reduced Parsons−Zobel slopes, ion−surface attraction can account for such an effect: an attractive interaction drives the ions closer to the interface than predicted in the Gouy−Chapman−Stern theory. This causes a decrease in the effective Debye length. The number of ions attracted to the interface thereby depends on the bulk ion concentration, causing an ion concentration-dependent increase in capacitance compared to the Gouy−Chapman−Stern predictions, as required for reproducing the experimentally measured reduced slopes in the Parsons−Zobel plots. We will therefore follow up on the idea of an attractive ion−surface interaction, trying to provide quantitative proof of whether this interpretation is realistic and extracting likely properties of the interaction based on a comparison of the model with experimental results.

2.2. Mean-Field Model with Ion Attraction. The Gouy−Chapman−Stern capacitance, eq 1, can be derived from a simple continuum model that allows for an analytic solution. More complex models of charged electrode−electrolyte interfaces can be constructed using more sophisticated local free energy functional-based continuum models. Such models allow for a changing dielectric constant $\varepsilon_r(x)$, for ion size effects, and they allow introducing a slowly varying ion−surface interaction $\varphi_i(x)$. In our model, we exploit this flexibility. In doing so, we follow closely ref 13, but the approach is quite generic and many similar approaches can be found in other publications (e.g., refs 14−17). In the following, we sketch this model in broad lines. More details can be found in Supporting Information in Section S1.

The double-layer capacitance is derived from the following local free energy expression[13]

https://doi.org/10.1021/acs.jpcc.1c02381
J. Phys. Chem. C 2021, 125, 16664−16673

$$\mathcal{F}[\rho_{\text{ions}}(x), \phi(x), \{c_i(x)\}] = \int \Bigg[-\frac{\varepsilon_r(x)}{8\pi} |\nabla\phi(x)|^2 + (\rho(x) + \rho_{\text{ions}}(x))\phi(x) + \sum_{i=1}^{p} c_i(x)\varphi_i(x) - \sum_{i=1}^{p} \mu_i(c_i(x) - c_i^0(x)) - T(s[\{c_i(x)\}] - s[\{c_i^0(x)\}]) \Bigg] dx \tag{3}$$

where the equation is given in atomic units and x defines the distance from the surface. The first two terms describe the electrostatic interaction created by the electric field $\phi(x)$, the ionic charge density [given by $\rho_{\text{ions}}(x) = \sum_{i=1}^{p} c_i(x) z_i$ with ion charge z_i and concentration c_i], and the charges on the metal interface $\rho(x)$. The third term describes the interaction of the aforementioned external potential $\varphi_i(x)$ with the ions.[18] The function $\varphi_i(x)$ can be repulsive, thereby simulating, for example, the Helmholtz plane. It can, however, also be attractive,[16,17,19] and we will exploit this in the present paper to account for an attractive ion−surface interaction. The fourth term accounts for a grand canonical description of the ions by taking their chemical potential μ_i into account. The last term is the entropic contribution to the free energy, where s is the entropy density. By inserting the entropy density obtained for a lattice gas model with an additional term for the solvent entropy[20−23] (see Supporting Information for details), ion size effects can be introduced in the model. The lattice gas model introduces a maximum ion density c_{max}, which is equal for all ions. In the present study, the effect of different ion sizes can thus only be included via a repulsive interaction in φ_i close to the surface. [Although extensions to this expression for unequal ion sizes exist,[14] we disregard them here, as they (at least some of them) are problematic due to sequence effects and/or their inability to capture realistic ion configurations in the state counting procedure.[24]]

From the free energy expression, eq 3, an expression for the local ion concentration, $c_i^{\text{MPB+int}}(x,\phi(x),\varphi(x))$, as a functional of the local electric and external potential can be derived by requiring $\frac{d\mathcal{F}}{dc_i} = 0$. This expression can be plugged into a modified Poisson−Boltzmann equation, obtained by minimizing the free energy $\mathcal{F}$ with respect to $\phi(x)$ (see Supporting Information for details)

$$\nabla\left(\varepsilon_r(x)\nabla\phi(x)\right) + 4\pi\sum_{i=1}^{p} z_i c_i^{\text{MPB+int}}(\phi(x)) = -4\pi\rho(x) \tag{4}$$

This second-order differential equation in the electrostatic potential $\phi(x)$ can be solved numerically for various different surface charge densities $\sigma = \int \rho(x)dx$, where $\rho(x)$ describes a distribution of charges located on the metal surface (see Supporting Information for further details on the numerical implementation). The potential difference $\phi = \phi(0) - \lim_{L\to\infty}\phi(L)$ can be considered as the electrode potential on a reference scale defined by the pzc of the electrode in the ideal Gouy−Chapman−Stern case. By numerically differentiating the resulting function $\sigma(\phi)$, we obtain the total differential capacitance of the interface

$$C = A\frac{d\sigma}{d\phi} \tag{5}$$

where A is the surface area. In the following, we use $A = 1$ cm^2 and report the capacitance in μF/cm^2.

Obviously, the resulting differential capacitance depends on the model parameters used in the free energy expression. While the full details on the model parameters and the functional forms of φ_i, ε_r, and ρ can be found in Supporting Information, Figure 3 summarizes the main model parameters used in this work: x_{rep} basically defines the distance of closest approach of the ions to the surface. At values $x < x_{\text{rep}}$, the external potential φ becomes large and positive, thus expelling any ions from this region. Together with the value of the relative permittivity $\varepsilon_r(x)$ close to the interface, x_{rep} influences the Helmholtz-type contribution to the differential capacitance by effectively shifting the Stern layer. The Gouy−Chapman-like contribution to the capacitance depends on the bulk ion concentration c^0 through eq 2. The contribution of ion−surface attraction to the capacitance depends on the parameters U_{att} and on $\Delta x = x_{\text{att}} - x_{\text{rep}}$ determining the attractive interaction strength and the distance over which ions are attracted to the surface. More sophisticated functional forms of the ion−surface interaction term defined by x_{rep}, x_{att}, U_{att}, and eq S8 in Supporting Information could be developed. However, we limit the expression to a simple (box-like) form in order to remain generic in the physical cause of the postulated attractive interaction. Finally, there is one parameter that influences all capacitive contributions: c_{max} defines the maximum ion concentration allowed, leading to ion crowding effects. Although c_{max} and x_{rep} are, in reality, likely coupled, we treat them as independent parameters here and keep c_{max}, and hence ion crowding effects, the same for all ion types.

By adjusting the various model parameters, different model interfaces can be simulated and the qualitative effect of an attractive ion−surface interaction can be studied. However, the mean-field model requires numerically solving eqs 4 and 5, hampering an easy interpretation of the results. In the next section, we therefore also develop an approximate, analytical capacitance model that can account for ion−surface attraction.

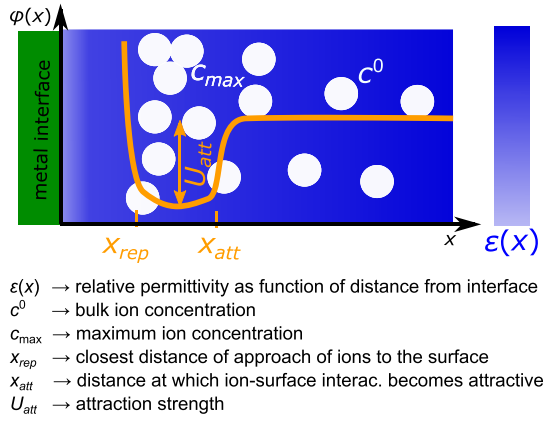

Figure 3. Schematic representation of the most important model parameters used in the continuum models. Parameters related to the ion−surface interaction are highlighted in orange and may differ for cations and anions.

https://doi.org/10.1021/acs.jpcc.1c02381
J. Phys. Chem. C 2021, 125, 16664−16673

2.3. Analytical Model. To allow for a more intuitive interpretation of the effects of ion−surface attraction on the capacitance, we make a few approximations to the mean-field model introduced above. These approximations allow us to derive a simplified, analytical capacitance model, similar to the Gouy−Chapman−Stern model. In contrast to the Gouy−Chapman−Stern model, however, our extended model allows accounting for an attractive ion−surface interaction via an additional concentration- and potential-dependent capacitive element C_{att} in parallel to the Gouy−Chapman capacitance

$$\frac{1}{C} = \frac{1}{C_H} + \frac{1}{C_{att} + C_{GC}} \tag{6}$$

as shown in Figure 1b.

Equation 6, as well as the functional form of C_{att}, can be derived as an approximation to the more generic mean-field model as follows: neglecting ion size effects, the expression for $c_i^{MPB+int}$, which follows from $\mathcal{F}$ and is given in eq S2 in Supporting Information, can be simplified to

$$c_i^{int}(x) = c_i^0 e^{-[z_i e_0 \phi(x) + \varphi_i(x)]/k_B T} \tag{7}$$

We simplify this expression further by assuming that (i) anions and cations are attracted to the surface by an interaction $\varphi = -U_{att}^{an/cat}$ in the interval $[x_{rep}, x_{att}] = [x_{rep}, x_{rep} + \Delta x]$ (see Figure 4) and that (ii) this interval is small compared to the Debye length, such that $\phi(x)$ (as generated by the double layer and the charges in the attractive region) does not change appreciably compared to the overall potential drop. In this case, $\phi^s = \phi(x_{att}) \approx \phi(x_{rep})$, and the ionic charges in the volume $V = \Delta x A$ can be written as

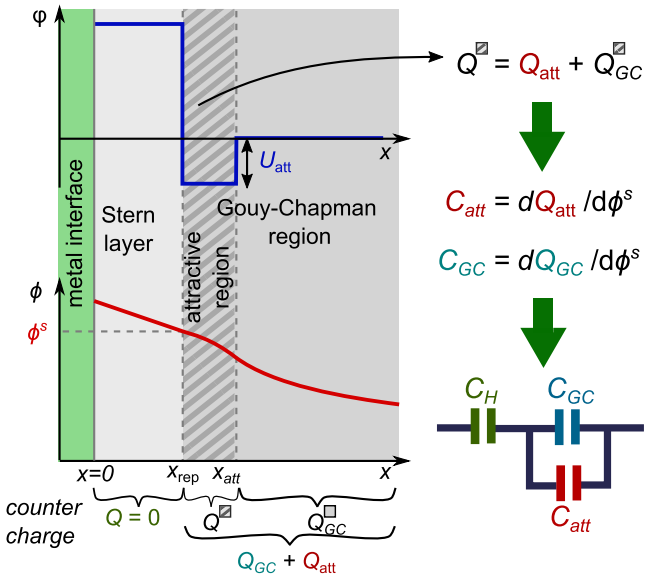

Figure 4. Graphical representation of the assumptions made in the derivation of the extended Gouy−Chapman−Stern + ion-attraction capacitance.

$$Q = e_0 c^0 A \Delta x [e^{-(ze_0\phi^s - U_{att}^{cat})/k_B T} - e^{-(-ze_0\phi^s - U_{att}^{an})/k_B T}] \tag{8}$$

where we assumed $z = z_{cat} = -z_{an}$ for simplicity. Q now captures all charges present in this region. From this quantity, we subtract those charges that would be there if the ion−surface attraction were zero. This way, we find the charges that are present exclusively due to the attractive interaction between ions and the electrode

$$Q_{att} = e_0 c^0 A \Delta x \left[e^{-ze_0\phi^s/k_B T} (e^{U_{att}^{cat}/k_B T} - 1) - e^{ze_0\phi^s/k_B T} (e^{U_{att}^{an}/k_B T} - 1) \right] \tag{9}$$

Differentiating this expression with respect to ϕ^s and taking into account that Q_{att} denotes countercharges (giving an additional negative sign), the ion−surface attraction capacitance C_{att} can be found as

$$C_{att}(\phi^s) = c^0 \cdot A \Delta x \frac{e_0^2 z^2}{k_B T} \left[(e^{U_{att}^{an}/k_B T} - 1) e^{ze_0\phi^s/k_B T} + (e^{U_{att}^{cat}/k_B T} - 1) e^{-ze_0\phi^s/k_B T} \right] \tag{10}$$

This attraction capacitance is proportional to the bulk ion concentration c^0 and depends on the potential ϕ^s.

Under the assumption that the attractive region is situated right next to the Stern layer (as depicted in Figure 4), ϕ^s is equivalent to the potential at the outer Helmholtz plane. In this case, both C_{GC} and C_{att} are functions of ϕ^s and the two capacitors should be considered as being in parallel, such that their charges add up, as required by eq 8 and the definition of Q_{att}.

Our analytic model predicts the ion−surface attraction capacitance to lie in parallel to the Gouy−Chapman capacitance. This deserves a comment, as most interface models consider the effect of ion adsorption as part of the inner layer capacitance[25−29] and hence in series with the Gouy−Chapman capacitance. To a certain extent, this may be due to geometric considerations: in Langmuir- or Frumkin-type (specific) adsorption models, the ions are considered to adsorb *within* the inner layer. In our case, however, such geometric considerations are not so plausible: our model is not a model for specific (chemical) adsorption. Instead, we want to capture a more generic attractive interaction. In fact, we believe that a relatively broad region of attraction and a rather diffuse ion−surface interaction are more in line with the absence of site blockage and specific adsorption in the experiments,[5,7] as well as with the very fast ad- and desorption of ions observed for weakly binding electrolytes on gold.[9] We therefore do not necessarily expect the ions to reside any closer to the interface than the "normal" solvated ions, which makes it seem less necessary to incorporate the effect of ion−surface attraction into the inner layer capacitance. Ultimately, however, the parallel capacitance model we suggest here is justified by its good correspondence with the predictions of the mean-field theory (as demonstrated in the next section), which, in fact, also holds when the ions are allowed to come very close to the surface—thus simulating, to a certain extent, adsorption on the surface, albeit (in the analytical model) without being able to capture a maximum coverage. Finally, the value obtained for U_{att} via fits to experiment turns out to be weaker than strong chemically specific adsorption would require (see Section 3.2).

Having developed a model that allows us to include ion−surface attraction, we are now in a position to (i) validate our simple analytical model against the more sophisticated mean-field model and (ii) to investigate the influence of various parameters on the model predictions in order to extract information on the interaction based on a comparison with experimental data.

https://doi.org/10.1021/acs.jpcc.1c02381
J. Phys. Chem. C 2021, 125, 16664−16673

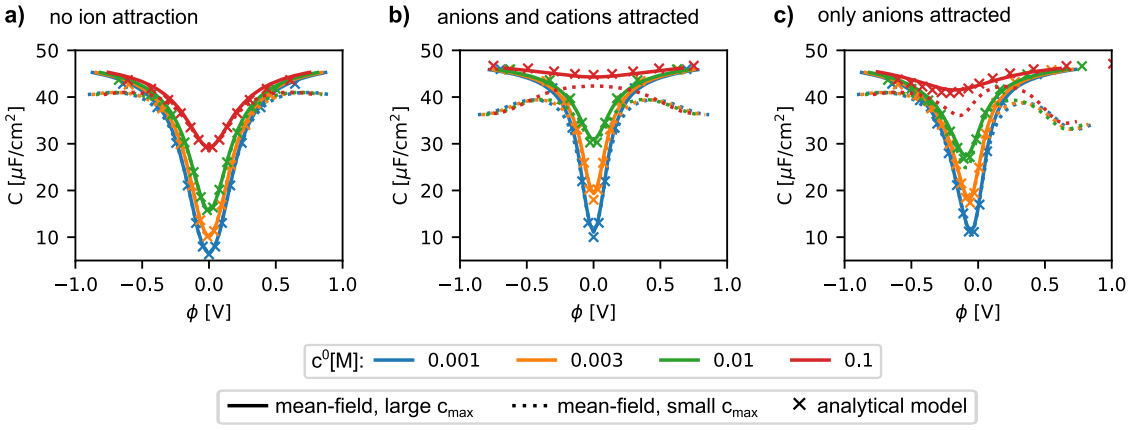

Figure 5. Comparison of capacitance curves obtained using the mean-field model [eqs 4 and 5] and the simplified analytical expression [eqs 6 and 10]: (a) no ion attraction; (b) anions and cations are both attracted to the interface; and (c) only anions are attracted to the interface. See Section S6 in Supporting Information for a full specification of the model parameters.

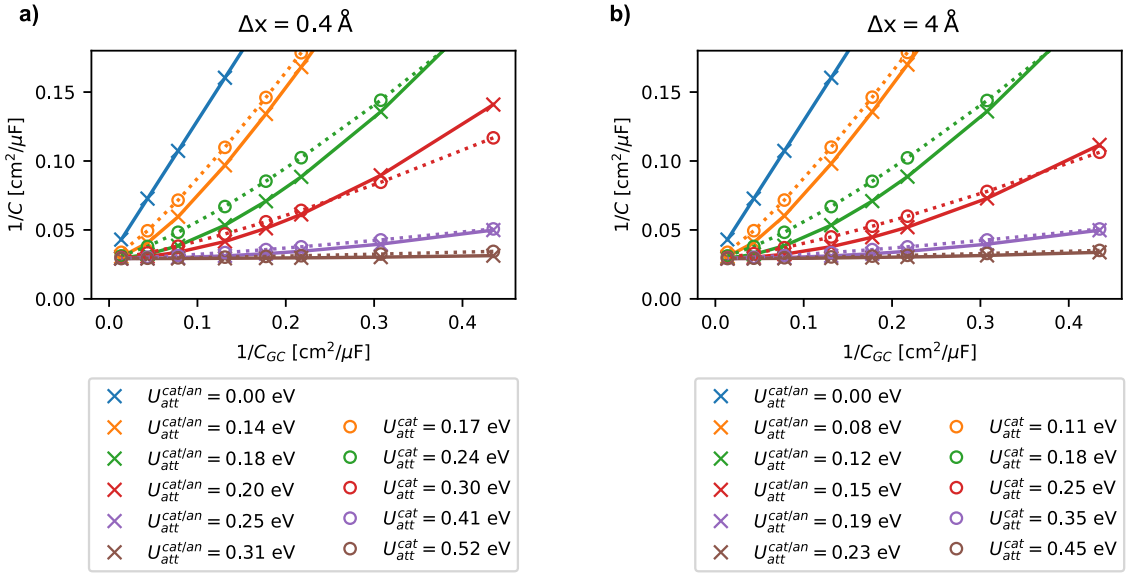

Figure 6. Parsons–Zobel plots obtained (a) for $\Delta x = 0.4$ Å and $C_H = 34\ \mu F/cm^2$ and (b) for $\Delta x = 4.0$ Å and $C_H = 34\ \mu F/cm^2$. Solid lines: $U_{att}^{an} = U_{att}^{cat}$; dotted lines $U_{att}^{an} = 0$ (in all cases, the capacitance obtained at the capacitance minimum is plotted).

3. RESULTS

3.1. Validity of the Analytical Model. The analytical model is a helpful tool as it provides a more intuitive understanding of the main processes involved in our double-layer model with ion–surface attraction than the numerical model. We validate our approximate analytical model with ion–surface attraction by comparing it to the predictions from the mean-field model. As shown in Figure 5, our analytical model is capable of reproducing the results from the mean-field model over a wide range of parameters. This is true not only for the Gouy–Chapman–Stern case (panel a) but also when both ions are attracted to the interface $[U_{att}^{cat} = U_{att}^{an}]$ (panel b) and when only cations (or anions) are attracted to the interface $[U_{att}^{an} = U$ and $U_{att}^{cat} = 0]$ (panel c). As expected, the analytical model cannot account for ion crowding effects captured by a low value of c_{max} (dotted lines), but as long as c_{max} is large enough, the potential ϕ is close to pzc $\phi(q = 0)$, and the ion concentration caused by ion–surface attraction is not too high; the model captures the predictions by the mean-field model well. In particular, also the minimum capacitance $C(\phi_{min})$ and the potential ϕ_{min} at which it occurs are captured correctly at low concentrations. As $C(\phi_{min})$ and ϕ_{min} are the observables that are used in this paper to compare the model predictions to experimental results (see the list of experimental results in the Introduction section), this is of particular importance for our purpose.

The capacitance minimum ϕ_{min} occurs at $\phi = 0$ in the Gouy–Chapman–Stern case as long as the bulk ion concentration is low enough such that the capacitance is dominated by C_{GC}. The same holds true of completely symmetric attraction of anions and cations to the surface. However, for $U_{att}^{cat} \neq U_{att}^{an}$ (and for $x_{rep}^{cat} \neq x_{rep}^{an}$), ϕ_{min} will differ from zero. Within the analytical model, the minimum in capacitance can be found analytically by solving for $dC/d\phi|_{\phi_{min}} = 0$. As shown in Supporting Information, this leads to a fourth order polynomial in ϕ_{min}^{s}, which can be solved numerically. This allows for a fast extraction of $C(\phi_{min})$ and its location ϕ_{min} without the need to compute the entire capacitance curve—a property that we will use in the following and that can be useful when trying to interpret experiments based on the model proposed here.

3.2. Attractive Ion–Surface Interaction as a Cause for the Experimental Findings on Pt. The first question we want

https://doi.org/10.1021/acs.jpcc.1c02381
J. Phys. Chem. C 2021, 125, 16664–16673

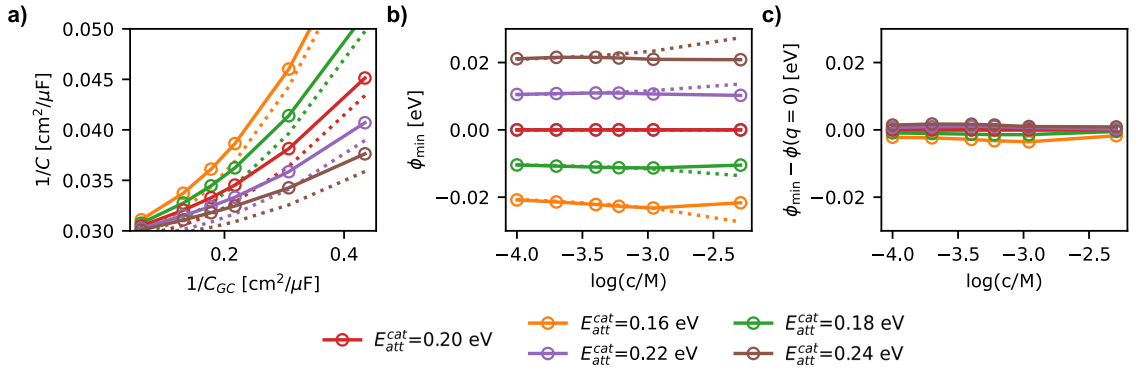

Figure 7. Both ions attracted to the surface but with different attraction strengths: (a) Parsons−Zobel plot, (b) potential of minimum capacitance, and (c) its offset from $\phi(q = 0)$ as a function of bulk ion concentration c^0. Dotted lines: results from the analytical model with $\Delta x = 4$ Å and $C_H = 34\ \mu$F. $U_{att}^{an} = 0.20$ eV in all cases [see Supporting Information, Section S6 for further specification of the model parameters. Results reported in (b,c) are converged to within a few meV. In (a), we keep the same *y*-axis scaling as in Figure 2b to allow for easier comparison of the slopes].

to answer is whether the capacitance model with ion−surface attraction is capable of capturing the experimental observations summarized in the Introduction section and thus whether the interpretation of the experimental results as a consequence of ion−surface attraction is reasonable. In answering this question, we will automatically touch on the second question phrased in the Introduction section, namely, which statements we can make on the ion−surface attraction based on a comparison of the model predictions with the experimental results.

We first investigate whether the model predicts a reduced Parsons−Zobel slope in the presence of ion−surface attraction and will move to the other experimental observations listed in the Introduction section later on. To this end, we compute the capacitance predicted by our analytical model, eqs 6 and 10, for various different ion−surface interaction strengths $U_{att}^{an/cat}$ and for different attractive regions Δx. The resulting Parsons−Zobel plots are shown in Figure 6. In panel a, we show results for a narrow region of ion−surface attraction (Δx = 0.4 Å), while panel b shows the corresponding results for a much broader region of ion−surface attraction (Δx = 4.0 Å). We also distinguish two limiting cases: (i) only one type of ion is attracted to the surface (solid lines) and (ii) both anions and cations are attracted to the surface in exactly the same way (dotted lines). As many of the parameters (e.g., Δx and U_{att}) are correlated, we refrain from attempting to fit the experimental data. Instead, we investigate the model predictions for a whole range of parameters. As shown in Figure 6, Parsons−Zobel slopes similar to the slopes obtained experimentally for Pt(111) (purple lines) can be obtained in all cases by tuning the ion−surface interaction strength. The interaction strength necessary to achieve such an effect is thereby on the order of only a few tens of meV, independent of whether Δx is very narrow or very broad and on whether only anions or anions and cations are attracted to the surface. Additionally, any interaction strength that is stronger by only 10 meV (brown lines) leads to Parsons−Zobel slopes significantly smaller than those observed experimentally on Pt(111) for $NaClO_4$, $KClO_4$, $CsClO_4$, LiF, and CH_3SO_3Na (see Figure 2b). As other parameters (such as ε_r or the width of the Helmholtz plane r_{rep}) have no influence on this observation, we can make the important observation that our model predicts the ion−surface interaction to be weak and to be largely independent of the ionic species used in the electrolyte. Keeping this in mind, we will try to extract more information on the ion−surface interaction on Pt(111) by analyzing the different parametrizations in more detail.

Historically, it is more common to assume that only one type of ion, namely, the anions, is attracted to the surface, while cations are usually assumed not to interact with the surface due to their strong solvation shell. Naively, one may want to discard the idea of "anion-only" attraction based on the fact that ϕ_{min} does not shift in a $KClO_4$ electrolyte and is close to pzc independently of ionic strength. However, as shown in the Supporting Information in Section S4, while this is a valid argument if the Helmholtz capacitance were small (on the order of 20 μF/cm^2), our model predicts negligible shifts of ϕ_{min} from pzc if the Helmholtz capacitance is large [as is indeed observed for Pt(111)].[5] Based on this argument, "anion-only" adsorption can thus not be ruled out. However, we dismiss this option of anion-only attraction in the following: for anion−surface attraction only, our model is not capable of reproducing the fourth experimental observation stated in the Introduction section, namely, that $\phi_{min}(c^0)$ can shift to higher and lower potentials depending on the cation identity in the electrolyte. When only anions are attracted to the surface, the model always predicts a negative shift of ϕ_{min} for increasing ionic strength. According to our model and its comparison to experimental results, "anion-only" adsorption thus does not seem to be a reasonable explanation.

The ion−surface interaction could also be present for both anions and cations. Symmetric cation and anion interaction with the surface could be mediated, for example, by image charge interactions. The effect of such a symmetric ion−surface interaction on the Parsons−Zobel plots has already been shown in Figure 6 (full lines). In contrast to the Parsons−Zobel slopes for anion−surface attraction only, the Parsons−Zobel plots for symmetric ion−surface interaction display a slight curvature. This behavior is expected as C_{GC} is proportional to $\sqrt{c^0}$, while C_{att} is proportional to c^0 according to eq 10. This leads to a slope that is dominated by C_{att} for large c^0 (i.e., small values of $1/C_{GC}$) and by C_{GC} for small c^0 (i.e., large values of $1/C_{GC}$). At very low ion concentrations, all curves for equal cation and anion−surface interaction thus tend toward a slope of 1. This asymptotic behavior may not be visible in the data range plotted, though. The experimental data obtained for Au(111) seem to suggest that no such curvature should be present (see Figure 2). For Pt(111), however, the curved lines predicted by the model actually provide a slightly better fit to the experimental data than a linear fit would. In the absence of more data, for example, for Au(111) at lower concentrations, we will thus accept this slight curvature in the Parsons−Zobel plots

https://doi.org/10.1021/acs.jpcc.1c02381
J. Phys. Chem. C 2021, 125, 16664−16673

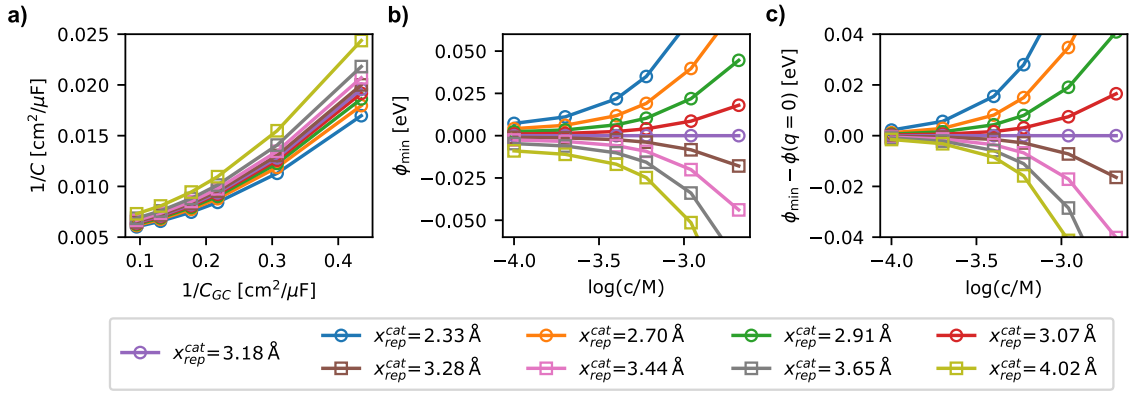

Figure 8. Both ions attracted to the surface but with different ion sizes: (a) Parsons−Zobel plot, (b) potential of minimum capacitance, and (c) its shift from $\phi(q = 0)$ as a function of bulk ion concentration c^0. $U_{att}^{an} = U_{att}^{cat} = 0.22$ eV, $x_{rep}^{an} = 3.18$ Å, and $x_{att}^{cat} = x_{att}^{an} = 5.29$ Å in all cases [see Supporting Information, Section S6 for further specification of the model parameters. In (a), we keep the same *y*-axis scaling as in Figure 2b to allow for easier comparison of the slopes].

as tentatively in line with the experimental data shown in the Parsons−Zobel plots and turn to investigate whether the model predictions also conform to the other experimental observations.

The remaining experimental observations (number two to four) concern measurements involving various different electrolytes ($LiClO_4$, $NaClO_4$, $CsClO_4$, LiF, and CH_3SO_3Na). Therefore, we first need to find a possibility to describe the effect of different electrolytes within our model.

Assuming that both anions and cations are attracted to the surface, the effect of different electrolytes can be mimicked by changing the relative attraction strength of anions and cations ($U_{att}^{an} \neq U_{att}^{cat}$) or by changing the geometric parameters of the ion−surface interaction ($x_{rep}^{an} \neq x_{rep}^{cat}$). The first case is shown in Figure 7, where we vary U_{att}^{cat} between 16 and 24 meV, while keeping U_{att}^{an} constant at 20 meV. The range of U_{att} is thereby chosen such that the resulting Parsons−Zobel slopes (panel a) correspond approximately to those obtained experimentally for Pt(111) in contact with various electrolytes. Within this range of values for U_{att}^{cat} versus U_{att}^{an}, our model predicts only small offsets of ϕ_{min} from $\phi(q = 0)$ (panel c), consistent with the experimental observations [exp. observation nr. 2: number two (ϕ_{min} is close to pzc)]. In this case however, our model also predicts negligible shifts of ϕ_{min} for increasing bulk ion concentration (see panel b). Experimentally, however, shifts of ϕ_{min} of several tens of meV have been observed, depending on the electrolyte (exp. observation nr. 4). This observation also holds when changing other parameters in the model, such as increasing the Helmholtz capacitance (see Figure S5 in the Supporting Information) and using a small value of c_{max} (see Figure S6 in the Supporting Information). As the present model (anions and cations are attracted to the surface but with slightly different attraction strengths) cannot capture all the experimental observations, it is also unlikely that the present model captures the main physics behind the attractive ion−surface interaction. We therefore turn to the second possibility: both cations and anions are attracted to the surface, but depending on the ion identity, the ions can access the surface more or less closely.

By changing x_{rep} for anions versus cations, we can allow cations to penetrate a different region (e.g., closer or further away from the surface) than anions. This allows us to capture the effect of different cation sizes as a consequence of different (hydrated) ion sizes. In Figure 8, we show results for $x_{rep}^{cat} = x_{rep}^{an} \pm 0.8$ Å. Our hypothetical (hydrated) cations can thus be smaller or larger than the hydrated anions by 0.8 Å. This range is somewhat arbitrary but is inspired by the range of hydrated ion radii (3.8−3.2 Å for Li^+ to Cs^+ from corrected Stokes radii[30] or 5.8−3.5 Å for Li^+ to Cs^+ extracted from double-layer capacitance measurements[31]). Within this range, the slope of the resulting Parsons−Zobel plots is basically unaffected (see Figure 8, panel a, where only results from the mean-field model are shown as our simplified analytical model does not allow for different ion sizes). Additionally, this difference in ion size between cations and anions does not cause a strong offset of ϕ_{min} from pzc, $\phi(q = 0)$, consistent with experimental observation number 2. Furthermore, ϕ_{min} starts to shift to more positive potentials when increasing the bulk ion concentration, if the hydrated cation is smaller than the anion (circles in panel b), while it shifts to more negative potentials, if the cation is larger than the anion (squares). This prediction is consistent with experimental observation number 4 (ϕ_{min} shifts toward more positive potentials in $CsClO_4$ and to more negative potentials in $LiClO_4$): as Cs^+ has a relatively small hydrated ion radius, $CsClO_4$ can be expected to correspond to a situation in which the cation is smaller than the anion (circles, positive shifting), while Li^+ has a relatively large hydrated ion radius, corresponding to the case shown in squares (negative shifting). These observations are robust with respect to changes in other model parameters (see Figures S7 and S8 in Supporting Information).

We may thus conclude that within the validity of our model, the comparison of model predictions and experimental observations suggests that both cations and anions are attracted to the surface with similar attraction strength but that they can access the surface to various degrees depending on the ion identity, leading to a shift in ϕ_{min} as a function of ionic strength.

4. DISCUSSION AND OUTLOOK

In the previous section, we presented a model that is capable of explaining several features of the double-layer capacitance on Pt(111). This includes the slopes observed in the Parsons−Zobel plots for Pt(111) and Au(111), which are reduced compared to the predictions from Gouy−Chapman theory, and observations made for the location of the minimum in the capacitance. Obviously, the fact that a model fits experimental results cannot be seen as proof that the model captures the correct physics. Nevertheless, the good correspondence between our final model and experiment and the robustness of

https://doi.org/10.1021/acs.jpcc.1c02381
J. Phys. Chem. C 2021, 125, 16664−16673

our conclusions with respect to various parameters in the model allow us to conclude that an attractive ion−surface interaction is a realistic interpretation for the observations made experimentally. Furthermore, our model suggests the attractive interaction to

- be very similar in strength for all ions (at least for the ions tested experimentally[5,7])
- affect anions and cations, and
- depend on the hydrated ion radius.

These observations are at odds with the traditional interpretation of reduced Parsons−Zobel plots to be due to specific (chemical) adsorption of ions on the surface, as these interactions generally depend strongly on the chemical species. Although the double-layer region of Pt(111) is narrow, adsorption and desorption of H^+ and OH^- (which would be present in *all* electrolytes) cannot explain the reduced Parsons−Zobel slopes, as this process does not depend on the electrolyte concentration, while a reduction of the Parsons−Zobel slopes requires such a dependency.

An explanation for an attractive ion−surface interaction could be a water-mediated ion−surface interaction. However, such an interaction would be expected to be more specific (i.e., ion-dependent) than what is suggested by the experimental results.

Yet another source of an attractive ion−surface interaction is the image charge effect. For $\varepsilon_r = 10$ close to the surface and ions residing 3 Å from the image plane, the image charge interaction is, however, only 12 meV. This is considerably weaker than the interaction strength predicted within the current model to be necessary to obtain slopes in the Parsons−Zobel plots comparable to those obtained for Pt(111). A very low relative permittivity (as can be caused by a strong water−Pt interaction), as well as an anomalously short image plane−ion distance, could increase this interaction. The former explanations (low ε_r) seems to be at odds with the large Helmholtz capacitance found for Pt(111).[5] However, the large Helmholtz capacitance observed on Pt(111) may also be a consequence of field-dependent water adsorption, as suggested in ref 11, leaving strong image charge interactions due to a low ε_r as possible explanation.

Clearly, the conclusions made above about the nature of the ion−surface interaction are based on a rather simple model. One may therefore wish to test whether the predictions hold when going to a higher level of theory, such as classical density functional theory for hard sphere fluids. While a higher level theory may strengthen the conclusions made, a proof for the interpretation of ion−surface interaction as a cause for the experimental results, as well as its characteristics, must rely on explaining the origin of the attraction, for example, by molecular dynamics calculations. Further verification or refutation of the hypothesis of the suggested model could, however, also come from experimental investigations: by studying even lower ion concentrations on Au(111), one could check whether the slope in the Parsons−Zobel plots increases toward 1, as predicted by the model for symmetric ion−surface attraction. A second check would be to investigate the double-layer capacitance for different electrolytes on gold: as shown in Figure S9 in Supporting Information, no shift in the potential of minimum capacitance is predicted for different electrolytes in this case because of the weaker interaction.

5. CONCLUSIONS

In this paper, we discussed properties of the double-layer capacitance of Pt(111) based on a comparison of experimental results with model predictions. To this end, we presented a double-layer model with an attractive ion−surface interaction and derived an approximation thereof, in which the attractive ion−surface interaction is captured by an additional "ion attraction capacitance" circuited in parallel to the Gouy−Chapman capacitance. The proposed model is capable of capturing several experimental observations[5,7] made for the double-layer capacitance of Pt(111) in contact with dilute electrolytes, including the fact that the Parsons−Zobel slope is strongly reduced, while the potential of minimum capacitance is nearly constant and close to pzc. By comparing various different model predictions with experimental results,[5,7] we thereby inferred likely properties of the ion−surface attraction. Based on this comparison, we conjecture that the various ions, including both anions and cations, are attracted to the Pt surface with a weak, but similarly strong interaction strength of a few tens of meV. This prediction is at odds with the traditional interpretation of specific (chemical) adsorption as the source of the attractive ion−surface interaction, as chemical adsorption is typically strongly dependent on the ionic species. The comparison of experimental results with model predictions furthermore suggests that the attractive interaction is counteracted by a repulsive force based on the (ion-dependent) distance of closest approach, which is determined by the hydrated ion radius.

Taken together, our results thus allow us to conclude that the interpretation of the strongly reduced Parsons−Zobel slopes observed for Pt(111) as being due to ion−surface attraction is realistic, even in view of other experimental observations, which suggest a nonexisting or very weak interaction (such as the nonshifting potential of minimum capacitance and the absence of experimentally measurable site blockage). Furthermore, our model has allowed us to make predictions on the nature of the interaction. In the case of the Pt(111) surface studied here, these predictions suggest that a reinterpretation of the traditional picture of specific (chemical) contact adsorption as the only or main source of ion−surface attraction may have to be reconsidered and we hope that these results trigger future work on the ion−surface interaction on Pt and other metals.

■ ASSOCIATED CONTENT

Supporting Information

The Supporting Information is available free of charge at https://pubs.acs.org/doi/10.1021/acs.jpcc.1c02381.

> Mean-field model: details; extracting the minimum capacitance for $U_{att}^{an} \neq U_{att}^{cat}$; relation of pzfc, pztc, and pme to ϕ and the surface charge q; anion-only and cation-only attraction to the surface; cations and anions attracted to the surface−additional information; and model parameters used for the figures (PDF)

■ AUTHOR INFORMATION

Corresponding Authors

Katharina Doblhoff-Dier − *Leiden Institute of Chemistry, Leiden University, Leiden 2300 RA, The Netherlands;* orcid.org/0000-0002-5981-9438; Email: k.doblhoff-dier@lic.leidenuniv.nl

https://doi.org/10.1021/acs.jpcc.1c02381
J. Phys. Chem. C 2021, 125, 16664−16673

Marc T. M. Koper − *Leiden Institute of Chemistry, Leiden University, Leiden 2300 RA, The Netherlands*; Email: m.koper@lic.leidenuniv.nl

Complete contact information is available at: https://pubs.acs.org/10.1021/acs.jpcc.1c02381

Notes

The authors declare no competing financial interest.

■ ACKNOWLEDGMENTS

The authors acknowledge Thom Hersbach for a critical reading of the manuscript.

■ REFERENCES

(1) Grahame, D. C. Differential Capacity of Mercury in Aqueous Sodium Fluoride Solutions. I. Effect of Concentration at 25°. *J. Am. Chem. Soc.* **1954**, *76*, 4819−4823.
(2) Rotenberg, B.; Bernard, O.; Hansen, J.-P. Underscreening in Ionic Liquids: A First Principles Analysis. *J. Phys.: Condens. Matter* **2018**, *30*, 054005.
(3) Gavish, N.; Elad, D.; Yochelis, A. From Solvent-Free to Dilute Electrolytes: Essential Components for a Continuum Theory. *J. Phys. Chem. Lett.* **2018**, *9*, 36−42.
(4) Zwanikken, J.; van Roij, R. Inflation of the Screening Length Induced by Bjerrum Pairs. *J. Phys.: Condens. Matter* **2009**, *21*, 424102.
(5) Ojha, K.; Arulmozhi, N.; Aranzales, D.; Koper, M. T. M. Double Layer at the Pt(111)-Aqueous Electrolyte Interface: Potential of Zero Charge and Anomalous Gouy-Chapman Screening. *Angew. Chem., Int. Ed.* **2020**, *59*, 711−715.
(6) Pajkossy, T.; Kolb, D. M. Double Layer Capacitance of Pt(111) Single Crystal Electrodes. *Electrochim. Acta* **2001**, *46*, 3063−3071.
(7) Ojha, K.; Doblhoff-Dier, K.; Koper, M. T. M. **2021** In preparation.
(8) Parsons, R.; Zobel, F. G. R. The Interphase between Mercury and Aqueous Sodium Dihydrogen Phosphate. *J. Electroanal. Chem.* **1965**, *9*, 333−348.
(9) Eberhardt, D.; Santos, E.; Schmickler, W. Impedance Studies of Reconstructed and Non-Reconstructed Gold Single Crystal Surfaces. *J. Electroanal. Chem.* **1996**, *419*, 23−31.
(10) Foresti, M. L.; Guidelli, R.; Hamelin, A. A Model for the Effect of Roughness of Single-Crystal Electrodes on Parsons-Zobel Plots. *J. Electroanal. Chem.* **1993**, *346*, 73−83.
(11) Le, J.-B.; Fan, Q.-Y.; Li, J.-Q.; Cheng, J. Molecular Origin of Negative Component of Helmholtz Capacitance at Electrified Pt(111)/Water Interface. *Sci. Adv.* **2020**, *6*, No. eabb1219.
(12) Bouzid, A.; Pasquarello, A. Atomic-Scale Simulation of Electrochemical Processes at Electrode/Water Interfaces under Referenced Bias Potential. *J. Phys. Chem. Lett.* **2018**, *9*, 1880−1884.
(13) Nattino, F.; Truscott, M.; Marzari, N.; Andreussi, O. Continuum Models of the Electrochemical Diffuse Layer in Electronic-Structure Calculations. *J. Chem. Phys.* **2019**, *150*, 041722.
(14) Baskin, A.; Prendergast, D. Exploring Chemical Speciation at Electrified Interfaces Using Detailed Continuum Models. *J. Chem. Phys.* **2019**, *150*, 041725.
(15) Melander, M. M.; Kuisma, M. J.; Christensen, T. E. K.; Honkala, K. Grand-Canonical Approach to Density Functional Theory of Electrocatalytic Systems: Thermodynamics of Solid-Liquid Interfaces at Constant Ion and Electrode Potentials. *J. Chem. Phys.* **2019**, *150*, 041706.
(16) Uematsu, Y.; Netz, R. R.; Bonthuis, D. J. The Effects of Ion Adsorption on the Potential of Zero Charge and the Differential Capacitance of Charged Aqueous Interfaces. *J. Phys.: Condens. Matter* **2018**, *30*, 064002.
(17) Baskin, A.; Prendergast, D. Improving Continuum Models to Define Practical Limits for Molecular Models of Electrified Interfaces. *J. Electrochem. Soc.* **2017**, *164*, E3438−E3447.
(18) Jinnouchi, R.; Anderson, A. B. Electronic Structure Calculations of Liquid-Solid Interfaces: Combination of Density Functional Theory and Modified Poisson-Boltzmann Theory. *Phys. Rev. B: Condens. Matter Mater. Phys.* **2008**, *77*, 245417.
(19) Uematsu, Y.; Netz, R. R.; Bonthuis, D. J. Analytical Interfacial Layer Model for the Capacitance and Electrokinetics of Charged Aqueous Interfaces. *Langmuir* **2018**, *34*, 9097−9113.
(20) Borukhov, I.; Andelman, D.; Orland, H. Steric Effects in Electrolytes: A Modified Poisson-Boltzmann Equation. *Phys. Rev. Lett.* **1997**, *79*, 435−438.
(21) Borukhov, I.; Andelman, D.; Orland, H. Adsorption of large ions from an electrolyte solution: a modified Poisson-Boltzmann equation. *Electrochim. Acta* **2000**, *46*, 221−229.
(22) Bazant, M. Z.; Kilic, M. S.; Storey, B. D.; Ajdari, A. Towards an Understanding of Induced-Charge Electrokinetics at Large Applied Voltages in Concentrated Solutions. *Adv. Colloid Interface Sci.* **2009**, *152*, 48−88.
(23) Bikerman, J. J. XXXIX. Structure and capacity of electrical double layer. *London, Edinburgh Dublin Philos. Mag. J. Sci.* **1942**, *33*, 384−397.
(24) Zhang, Y.; Huang, J. Treatment of Ion-Size Asymmetry in Lattice-Gas Models for Electrical Double Layer. *J. Phys. Chem. C* **2018**, *122*, 28652−28664.
(25) Grahame, D. C.; Soderberg, B. A. Ionic Components of Charge in the Electrical Double Layer. *J. Chem. Phys.* **1954**, *22*, 449−460.
(26) Grahame, D. C. Components of Charge and Potential in the Non-diffuse Region of the Electrical Double Layer: Potassium Iodide Solutions in Contact with Mercury at 25°1. *J. Am. Chem. Soc.* **1958**, *80*, 4201−4210.
(27) Grahame, D. C.; Parsons, R. Components of Charge and Potential in the Inner Region of the Electrical Double Layer: Aqueous Potassium Chloride Solutions in Contact with Mercury at 25°. *J. Am. Chem. Soc.* **1961**, *83*, 1291−1296.
(28) Damaskin, B.; Karpov, S.; Dyatkina, S.; Palm, U.; Salve, M. Differential capacity curves at adsorption of organic ions. *J. Electroanal. Chem. Interfacial Electrochem.* **1985**, *189*, 183−194.
(29) Damaskin, B. B.; Stenina, E. V.; Sviridova, L. N. Modified Model of Electrical Double Layer for Mixed Solutions of Constant Ionic Strength. *Russ. J. Electrochem.* **2010**, *46*, 374−382.
(30) Nightingale, E. R. Phenomenological Theory of Ion Solvation. Effective Radii of Hydrated Ions. *J. Phys. Chem.* **1959**, *63*, 1381−1387.
(31) Ringe, S.; Clark, E. L.; Resasco, J.; Walton, A.; Seger, B.; Bell, A. T.; Chan, K. Understanding Cation Effects in Electrochemical CO2 Reduction. *Energy Environ. Sci.* **2019**, *12*, 3001−3014.

■ NOTE ADDED AFTER ASAP PUBLICATION

This paper was published ASAP on July 21, 2021, with an error in eq 9 due to a production error. The corrected version was reposted on July 22, 2021.